Soft Matter

Accepted Manuscript

This is an *Accepted Manuscript*, which has been through the Royal Society of Chemistry peer review process and has been accepted for publication.

Accepted Manuscripts are published online shortly after acceptance, before technical editing, formatting and proof reading. Using this free service, authors can make their results available to the community, in citable form, before we publish the edited article. We will replace this *Accepted Manuscript* with the edited and formatted *Advance Article* as soon as it is available.

You can find more information about *Accepted Manuscripts* in the Information for Authors.

Please note that technical editing may introduce minor changes to the text and/or graphics, which may alter content. The journal's standard Terms & Conditions and the Ethical guidelines still apply. In no event shall the Royal Society of Chemistry be held responsible for any errors or omissions in this *Accepted Manuscript* or any consequences arising from the use of any information it contains.

ROYAL SOCIETY OF CHEMISTRY

www.rsc.org/softmatter

Title of the manuscript:

Testing the mean magnetization approximation, dimensionless and scaling numbers in magnetorheology

Authors:

José Antonio Ruiz-López, Juan Carlos Fernández-Toledano, Roque Hidalgo-Alvarez, Juan de Vicente*

Affiliation:

Department of Applied Physics, Faculty of Sciences, University of Granada, C/ Fuentenueva s/n, 18071-Granada, Spain

* jvicente@ugr.es

Submitted to Soft Matter

Soft Matter Accepted Manuscript

Abstract

The mean magnetization (MM) approximation is undoubtedly the most widely used approximation in magnetorheology both from a theoretical and simulation perspective. According to this, spherical magnetizable particles under field can be replaced by effective dipole moments m placed at their center with strength $m = V_p \langle M_p \rangle$. Here V_p and $\langle M_p \rangle$ are the volume and mean (average) magnetization of the particles, respectively. In spite of being extensively used, there is not a mathematical justification to do so in most cases. In this manuscript, we test this approximation using experiments, theories and simulations, for a wide range of magnetic field strengths and particle loadings, in both conventional magnetorheological fluids (CMRFs) and inverse ferrofluids (IFFs). Results demonstrate that the MM approximation is applicable in IFFs for a very wide range of field strengths (up to external fields of 265 kA/m) and particle loadings (up to 20 vol%). For CMRFs, the MM approximation is only applicable in two particular circumstances; in magnetic saturation or in infinite dilution.

Keywords

Magnetorheological fluids, inverse ferrofluids, dimensionless numbers, scaling curves, universal curves, magnetorheology.

Soft Matter Accepted Manuscript

1. Introduction

Generally speaking, magnetorheological (MR) fluids are non-Brownian magnetic field-responsive suspensions. There are essentially two kinds of MR fluids: i) conventional MR fluids (CMRFs) prepared by dispersion of magnetizable particles in a non-magnetic liquid carrier,[1] and ii) inverse ferrofluids (IFFs) prepared by dispersion of non-magnetic particles within a ferrofluid.[2-3] In the absence of magnetic fields, MR fluids behave as regular dispersions. However, in the presence of magnetic fields particles interact through magnetic forces eventually forming elongated structures in the field direction.[4-7]

Despite their different magnetization mechanisms, the mechanical (rheological) behavior of CMRFs and IFFs can be understood using the same principles -under the *Particle Magnetization Model*.[7] CMRFs are clearly preferred in commercial applications, while IFFs are considered model systems and generally used for fundamental studies.[5,6,8] The main reason for this is that magnetostatic interactions in IFFs are weak and the dispersed particles can be easily prepared with a very high monodispersity level.[4]

At large field strengths colloidal interactions do not play a role and, as a result, only two dimensionless numbers are needed to describe the rheology of MR fluids: the Mason number, Mn, and particle concentration, ϕ. Currently, the scaling with Mason number seems well understood. However, the understanding of the effect of particle loading is still incomplete.[7-10] Interestingly, the effect of particle concentration in the dimensionless shear viscosity (normalized by the high-shear viscosity) is solely

Soft Matter Accepted Manuscript

contained in the critical Mason number Mn^* (i.e. an apparent yield stress) that is associated to the transition from magnetostatic to hydrodynamic control.[8,11]

A major approximation that is commonly used in the description of MR fluids is the so-called mean (average) magnetization (MM) approximation. According to this, dispersed particles can be substituted by a magnetic dipole placed at their center. This approximation is not justified in most experimental cases and only becomes exact in two limiting scenarios: i) at low field strengths in dilute systems, and ii) in magnetic saturation. For a given particle concentration, the MM approximation has been successful in the description of the field dependence in CMRFs.[12,13] Also, the MM approximation has been successfully employed as well in the case of IFFs to ascertain the effect of particle loading on the MR performance. A linear dependence with volume fraction $Mn^* \propto \phi$ has been reported in very good agreement with analytical theories and experiments in the dilute regime.[8]

To the best of our knowledge, the MM approximation has not been exhaustively tested yet in the case of CMRFs and IFFs for different concentrations. The benefit of using this approximation with appropriate dimensionless numbers is that the effect of shear rate, field strength and particle concentration can be ascertained with only a few experimental measurements. Thus, in this work we aim to test the MM approximation using theoretical developments, particle level simulations and experimental data on CMRFs and IFFs for a wide range of field strengths (from the linear to nearly the saturation regime) and particle concentrations (from dilute to concentrated suspensions).

Soft Matter Accepted Manuscript

2. Mean magnetization (MM) approximation

Within the MM approximation, the interaction force between two spherical particles can be calculated in the equivalent problem of two dipoles located at the center of the spheres. In particular, a given particle (radius a, volume V_p) with average magnetization $\langle M_p \rangle$ is assimilated as a magnetic moment of strength:

$$m = V_p \langle M_p \rangle = \frac{4\pi}{3} a^3 \langle M_p \rangle \qquad [1]$$

In this work we will use $\langle M_p \rangle = M_{susp} / \phi$, where M_{susp} is the suspension magnetization and ϕ is the particle concentration.

The magnetostatic interaction force between two dipoles of strength m separated a distance r can be written as:

$$\begin{aligned} \vec{F} &= \frac{3\mu_0 \mu_{cr} m^2}{4\pi r^4} [(3\cos^2\theta - 1)\hat{r} + \sin(2\theta)\hat{\theta}] = \\ &= F_{mag} \left(\frac{2a}{r} \right)^4 [(3\cos^2\theta - 1)\hat{r} + \sin(2\theta)\hat{\theta}] \end{aligned} \qquad [2]$$

where θ is the angle formed between the center-to-center line and the magnetic field direction, μ_0 is the permeability of vacuum, μ_{cr} is the relative permeability of the continuous phase, and F_{mag} is a measure of the strength of the magnetostatic force. By substitution of Equation [1] in Equation [2] we get an expression for F_{mag} as a function of $\langle M_P \rangle$:

Soft Matter Accepted Manuscript

$$F_{mag} = \frac{1}{12}\pi\mu_0\mu_{cr}a^2\left\langle M_p\right\rangle^2 \quad [3]$$

As stated above, for MR fluids, the Lambda ratio (i.e. ratio between magnetostatic and thermal forces; $\lambda = \pi\mu_0\mu_{cr}a^3\left\langle M_p\right\rangle^2 \Big/ 18\kappa_B T$) is generally very large, and as a result their flow behavior is governed by only two dimensionless numbers: particle volume fraction ϕ and Mason number Mn.[7] The Mason number is defined as the ratio between the viscous shear forces, $F_{drag} = 6\pi\eta_c\dot{\gamma}a^2$, and the magnetostatic forces, F_{mag}. Here η_c stands for the viscosity of the continuous phase and $\dot{\gamma}$ is the magnitude of the shear rate tensor. It is important to remark that different considerations for F_{mag} lead to different definitions of the Mason numbers. Using Equation [3], the Mason number can be written as follows:

$$\mathrm{Mn} \equiv \frac{F_{drag}}{F_{mag}} = \mathrm{Mn}_{<\mathrm{M}>} = \frac{72\eta_c\dot{\gamma}}{\mu_0\mu_{cr}\left\langle M_p\right\rangle^2} \quad [4]$$

Improvements to Equations [3 and 4] for non-dilute suspensions involve the substitution of η_c (and μ_{cr}) by the viscosity (and permeability) of the suspensions as a whole. Interestingly, the use of Equation [4] permits the construction of scaling rheological curves also facilitating the modeling and simulation of these systems. Actually, Equation [4] has been successfully used in the past to collapse steady shear viscosity data for CMRFs[12,14,15] and IFFs[4].

Soft Matter Accepted Manuscript

However, in spite of being widely used, strictly speaking, the MM approximation is not applicable in most of the experimental data reported on MR fluids to date. The reason for this is that the MM approximation is only valid for homogeneous magnetic fields (i.e. generally speaking, exceedingly low concentrations) and/or magnetically saturated suspension (i.e. exceedingly large field strengths). On the one hand, the former condition is never realized in practice because MR fluids are never dilute by definition. On the other hand, the later condition is only guaranteed for sufficiently large magnetic field strengths and this is difficult to achieve because of field-induced particle migration and/or undesirable heating of the samples. In summary, most of the available data reported in the literature concern concentrated, non-saturated MR fluids and therefore, strictly speaking, the MM approximation is not applicable.

3. Validity of the MM approximation: Mason numbers and magnetic stress

3.1. Low fields and dilute suspensions

In the case of very low magnetic field strengths in dilute suspensions (i.e. within the linear magnetization regime), the magnetostatic interparticle force F_{mag} is proportional to the external magnetic field strength squared ($F_{mag} \propto H_0^2$) because $\langle M_p \rangle = 3\beta H_0$. Here $\beta = (\mu_{pr} - \mu_{cr})/(\mu_{pr} + 2\mu_{cr})$ is the contrast factor (or coupling parameter) and μ_{pr} is the relative permeability of the particles.

Under these conditions, it can be demonstrated that Equations [3 and 4] reduce to:[7]

Soft Matter Accepted Manuscript

$$F_{mag,L} = \frac{3}{4}\pi\mu_0\mu_{cr}\beta^2 a^2 H_0^2 \quad [5a]$$

$$\mathrm{Mn_L} = \frac{8\eta_c\dot{\gamma}}{\mu_0\mu_{cr}\beta^2 H_0^2} \quad [5b]$$

According to Equation [5a], the magnetic force between the particles comes from the permeability mismatch between the two phases, β. Interestingly, β is a function of the magnetic field strength. In the case of CMRFs β can take values between 0 (large fields) and 1 (low fields). In contrast, in the case of IFFs the contrast factor reduces to $\beta = (1-\mu_{cr})/(1+2\mu_{cr})$ and, as a consequence, β can take values between -0.5 (low fields) and 0 (large fields). Equation [5b] has been successfully used in the past to collapse steady shear viscosity data for low and intermediate (non-linear) magnetic field strengths in CMRFs,[11] IFFs,[6] and ER systems.[16]

When the magnetic field strength is further increased the suspensions approach to the saturation regime and Equations [5a and 5b] do not apply anymore. In particular, in this regime the magnetostatic interparticle force is no longer proportional to $\beta^2 H_0^2$ because the magnetization vector varies with position inside each interacting particle; in particular the magnetization in the polar regions begins to saturate (see Klingenberg[12] and references therein). FEM simulations carried out by Ginder and Davies[17] demonstrate that in this case the power law exponent of the magnetic field strength becomes smaller than 2.

Soft Matter Accepted Manuscript

3.2. Saturating fields

For very large magnetic field strengths the suspensions completely magnetize; $M_{susp} = M_{susp,sat}$. In the case of magnetically saturated suspensions the particles acquire a uniform magnetization within their volume, $M_{p,sat}$, and the MM approximation is truly applicable. Here $\langle M_p \rangle = M_{p,sat} = M_{susp,sat}/\phi$. In this case, Equations [3 and 4] become independent of the magnetic field strength and reduce to:[12]

$$F_{mag,sat} = \frac{1}{12}\pi\mu_0\mu_{cr}a^2M_{p,sat}^2 \quad [6a]$$

$$\mathrm{Mn}_{\mathrm{sat}} = \frac{72\eta_c\dot{\gamma}}{\mu_0\mu_{cr}M_{p,sat}^2} \quad [6b]$$

3.3. Magnetic stress scale

Starting from the expressions for the magnetostatic force in every field strength regime (linear and saturation), a magnetic stress τ_{mag} can be simply estimated by the ratio of the corresponding magnetostatic force (Equations [3, 5a and 6a]) divided by the particle area A_p. A simple estimation of A_p can be carried out if we assume a single-width particle chain like structuration. In this particular case, it can be demonstrated that $A_p \propto 2\pi a^2/3\phi$ (see Annex), and therefore the magnetic stress reads as follows:

$$\tau_{mag} \equiv \tau_{mag,<M>} = \frac{1}{8}\phi\mu_0\mu_{cr}\langle M_p \rangle^2 \quad [7a]$$

$$\tau_{mag,L} = \frac{9}{8}\phi\mu_0\mu_{cr}\beta^2H_0^2 \quad \text{Low fields (Linear)} \quad [7b]$$

$$\tau_{mag,sat} = \frac{1}{8}\phi\mu_0\mu_{cr}M_{p,sat}^2 \quad \text{Large fields (Saturation)} \quad [7c]$$

Soft Matter Accepted Manuscript

$\mu_{cr} \approx 1$ in the case of saturating fields for IFFs (e.g. see Figure 3b in reference 5).

At this point it is very important to emphasize that the particle area A_p expression assumes a single-width particle chain arrangement that is not necessarily the case in highly concentrated and strongly magnetized MR fluids where more complex structures appear. As a result, Equation [7] is only strictly applicable in the case of dilute MR fluids. Magnetostatic stresses given by Equation [7] physically correspond to a typical stress scale in terms of particle loading and magnetic field strengths. In the absence of other interparticle interactions, the magnetic stress, τ_{mag} will be proportional to the so-called yield stress, τ_y (i.e. the minimum stress required for the onset of flow).

4. Analytical theories

To model the rheological behavior of MR fluids, plastic analytical theories are generally employed. The Bingham model is undoubtedly the most widely used for steady shear flow. In dimensionless form it can be written as follows:

$$\frac{\eta}{\eta_\infty} = 1 + \frac{\mathrm{Mn}^*}{\mathrm{Mn}} \qquad [8]$$

where η_∞ is the (field-independent) high-shear viscosity and Mn^* is the critical Mason number. Mn^* essentially represents the apparent yield stress in the MR fluid. For a given concentration, if $\mathrm{Mn} < \mathrm{Mn}^*$ magnetostatic interactions predominate and the viscosity diverges. However, if $\mathrm{Mn} > \mathrm{Mn}^*$ hydrodynamic interactions predominate and the viscosity approaches to the high-shear viscosity. In general, assuming that other

Soft Matter Accepted Manuscript

colloidal interactions are small, the only dependence of the critical Mason number would be on the particle loading; $\mathrm{Mn}^* = \mathrm{Mn}^*(\phi)$. Microscopic models have been proposed in the literature to explain the critical Mason number dependence on the volume fraction: $\mathrm{Mn}^*(\phi) = C\eta_c\phi/\eta_\infty$ where C is a constant whose particular value depends on the particular assumptions or simplifications of the model.[4,18-20] According to these models a linear dependence with the volume fraction is expected for $\mathrm{Mn}^*(\phi)$ in the case of dilute suspensions because, in this case, $\lim_{\phi\to 0}\eta_\infty = \eta_c$. For larger concentrations a non-linear dependence would be expected and indeed a maximum with particle concentration could also appear (see below).

In spite of the success of the Bingham model, deviations from the Bingham model have also been described in the literature with regards to CMRFs and IFFs (e.g. see Ramos *et al.*[6] and references therein). In order to explain these discrepancies, a structural viscosity model was recently proposed by Berli and de Vicente:[11]

$$\frac{\eta}{\eta_\infty} = \left[\frac{1+(\mathrm{Mn}/\mathrm{Mn}^*)^{1/2}}{(\eta_\infty/\eta_0)^{1/2}+(\mathrm{Mn}/\mathrm{Mn}^*)^{1/2}}\right]^2 \qquad [9]$$

This model predicts a smoother transition between the magnetostatic and hydrodynamic regimes in the case of CMRFs and a low-shear viscosity plateau for IFFs. In the particular case of CMRFs, the low-shear plateau is not experimentally accessible because i) $\eta_0 >> \eta_\infty$ and ii) limited torque resolution of the rheometers. In this case, Equation [9] can be reduced to a dimensionless Casson-like equation:[11]

Soft Matter Accepted Manuscript

$$\eta/\eta_\infty = 1 + \left(\mathrm{Mn}/\mathrm{Mn}^*\right)^{-1} + 2\left(\mathrm{Mn}/\mathrm{Mn}^*\right)^{-1/2} \quad [10]$$

Interestingly, both Bingham and Casson models predict a divergent viscosity for low shear rates that corresponds to an apparent yield stress τ_y. This yield stress τ_y is related to the critical Mason number Mn^* as follows:

$$\mathrm{Mn}^* \equiv \mathrm{Mn}^*_{<\mathrm{M}>} = \frac{72\tau_y}{\mu_0\mu_{cr}\left\langle M_p \right\rangle^2}\frac{\eta_c}{\eta_\infty} \quad [11a]$$

$$\mathrm{Mn}_\mathrm{L}^* = \frac{8\tau_y}{\mu_0\mu_{cr}\beta^2 {H_0}^2}\frac{\eta_c}{\eta_\infty} \quad \text{Low fields (Linear)} \quad [11b]$$

$$\mathrm{Mn}_{\mathrm{sat}}^* = \frac{72\tau_y}{\mu_0\mu_{cr} {M_{p,sat}}^2}\frac{\eta_c}{\eta_\infty} \quad \text{Large fields (Saturation)} \quad [11c]$$

Starting from the Casson model, the dimensionless shear stress τ/τ_{mag} can be expressed, as a function of the critical Mason number Mn^* as follows:

$$\frac{\tau}{\tau_{mag}} = \frac{\eta_\infty}{9\phi\eta_c}\left(\mathrm{Mn}^* + \mathrm{Mn} + 2\mathrm{Mn}^{*1/2}\,\mathrm{Mn}^{1/2}\right) \quad [12]$$

In Equation 12, the first term is independent of the Mason number and, hence, independent of the shear rate (i.e. it is the apparent yield stress). Thus, the yield stress can be expressed scaled by the magnetic stress, $\tau_y/\tau_{mag} = \eta_\infty \mathrm{Mn}^*/9\phi\eta_c$. Micromechanical models[4,18-20] and experiments for IFFs[8] suggest that $\eta_\infty \mathrm{Mn}^*/\eta_c \propto \phi$, and therefore the ratio τ_y/τ_{mag} is independent on both the particle loading and the magnetic field strength. As a consequence, the magnetic stress τ_{mag} is a suitable scale

Soft Matter Accepted Manuscript

for the dipolar magnetostatic interactions and the particle volume fraction. Obviously, similar to Equation [10], a master curve can be obtained for the stress simply dividing by the yield stress:

$$\frac{\tau}{\tau_y} = 1 + \frac{\mathrm{Mn}}{\mathrm{Mn}^*} + 2\left(\frac{\mathrm{Mn}}{\mathrm{Mn}^*}\right)^{1/2} \qquad [13]$$

Equation 13 provides different curves for the different values of the critical Mason number. However, all these curves can be collapsed into only one curve if the Mason number is normalized by the critical Mason number. Thus, the knowledge of the magnetization of the suspension and the particle loading suffice to describe the rheology of the MR fluids under the assumptions considered.

5. Particle level simulations

Brownian molecular dynamic simulations were carried out in order to test the MM approximation. The simulation method was originally described in Fernández-Toledano *et al.*[21] and is now restricted to monodisperse particles (i.e. the particle diameter was fixed to σ). MR fluids were modeled by $N = 1000$ neutrally buoyant Hard Spheres in a Newtonian continuous medium. The system was confined between two parallel walls perpendicular to the field direction, z , and periodic boundary conditions were applied in the x and y direction. The system was subjected to a constant dimensionless temperature $T^* = 0.1$.

The Langevin equation involved contributions coming from interparticle magnetostatic interactions, hydrodynamic drag and short range repulsions. We assumed

Soft Matter Accepted Manuscript

pair-wise and point-dipole approximation to calculate magnetic forces. The dimensionless external magnetic field was fixed to $H_0^* = 150$. Hydrodynamic interactions were neglected and particles were subjected to an external flow by using Stokes' law. This approximation was used bearing in mind that the hydrodynamic stress is not the main contribution of the total stress as demonstrated in Lagger *et al*.[22] The friction coefficient was set as $\zeta^* = 722.1$. In order to avoid overlapping between particles and between a particle and the walls, short-range exponential repulsive forces were used. Exponential law forces were used instead of power law forces since the former promotes the formation of thick aggregates that are actually observed experimentally.[23,24]

The Langevin thermostat was switched-off in the direction of non-conservative forces. Therefore, the momentum is conserved in the shear direction while the temperature was conserved by applying the thermostat in the other directions.[21] Shear stress was calculated using the following equation at each time step:

$$\tau_{\alpha\beta} = -\frac{1}{V}\left(\sum_{i=1}^{N}\frac{p_i^{\alpha}p_i^{\beta}}{M_i} + \sum_{i\neq j} r_{ij}^{\alpha}F_{ij}^{\beta}\right) \qquad [14]$$

where $\tau_{\alpha\beta}$ is the α-β-component of the stress tensor, V is the volume of the simulation box, p_i^{α} and p_i^{α} are respectively the α and β-components of the linear momentum of the particle i, M_i is the mass of the particle i, r_{ij}^{α} is the α-component of the distance between a particle i and j and F_{ij}^{β} is the β-component of the total pair-wise interaction between the particle i and j.

Soft Matter Accepted Manuscript

Stress growth simulations were carried out under external magnetic fields. They consisted in three stages: First, the particles were randomly distributed in the simulation box. Secondly, the MR fluid was structured at rest (quiescent conditions) under the presence of magnetostatic interactions. Finally, a start-up test was initiated. The dimensionless shear rate was ranged between $\dot{\gamma}^* = 0.001$ and $\dot{\gamma}^* = 1000$ and the shear stress for each shear rate was calculated by averaging the large-strain values of the stress tensor over 500 configurations in the interval $\gamma \in [2,10]$ where the shear stress achieves an steady value. The time step was fixed as $\Delta t^* = 10^{-4}$. From start-up tests, full rheograms were first obtained and latter, the Equation [10] was fitted to the data to ascertain Mn^*.

6. Experimental

Two kinds of MR fluids were tested in this work. On the one hand, conventional MR fluids (CMRFs) prepared by dispersion of carbonyl iron microparticles (grade HQ from BASF SE Germany) in silicone oils ($\eta_c = 20 mPa \cdot s$ from Sigma-Aldrich). On the other hand we formulated inverse ferrofluids (IFFs) by dispersion of silica particles (obtained from Stöber method) in a commercial APG ferrofluid ($\eta_c = 44 mPa \cdot s$ from Ferrotech). Further details on the preparation and characterization of the IFFs can be found in Ruiz-López *et al.*[8]

Magnetic properties of carbonyl iron particles and ferrofluids were obtained by measuring their hysteresis cycles at room temperature in a Quantum Design (San Diego, CA) MPMS-XL 5.0 T magnetometer. The external magnetic field strength was varied from $4000 kA/m$ to $-4000 kA/m$. The magnetization curves of the suspensions were

Soft Matter Accepted Manuscript

also measured in order to calculate the mean magnetization of the particles to use the MM approximation. More details on the characterization of the ferrofluids used in this work can be found in Ramos *et al.*[6]

As stated above, the MM approximation is strictly valid only in the case of low fields at infinite dilution and at saturating fields. As a result, to test this approximation we decided to explore intermediate fields and concentrated suspensions. Magnetic fields investigated ranged $H_0 \in [17, 665]$ kA/m. Concentrations investigated were $\phi \in [0.01, 0.50]$ in the case of CMRFs and $\phi \in [0.10, 0.20]$ in the case of IFFs.

Steady shear flow curves were obtained in a commercial magnetorheometer (MCR 501 with the MRD70/1T magnetocell, Anton Paar) in plate-plate configuration (20 mm diameter, 300 microns gap). All tests were carried out in isothermal conditions (25 ºC). The protocol consisted as follows: (i) precondition at a constant shear rate of 100 s^{-1} for 30 s, (ii) the magnetic field is suddenly applied and the suspension is left to equilibrate for 1 min, (iii) the rheogram starts. Two kinds of tests were performed to obtain the rheograms either controlling the shear stress or the shear rate: (a) in the first test, the shear stress was logarithmically increased at a rate of 10 points/decade from 10^{-1} Pa to 10^5 Pa in the case of CMRFs and from 10^{-1} to 10^3 Pa in the case of IFFs. In the particular case of CMRFs, the stress range depended on the particle volume fraction. In all cases, the acquisition time was 5 s per data point and the test was stopped if the shear rate overpassed 10^3 s^{-1}; (b) in the second test, for CMRFs the shear rate was logarithmically increased at a rate of 10 points/decade from 10^{-2} to 10^4 s^{-1}. The acquisition time was 10 s per data point. Once the resulting shear rate in (a) or shear stress in (b) was measured, the *apparent* viscosity was calculated by dividing the

Soft Matter Accepted Manuscript

applied shear stress by the shear rate, calculated at the rim of the plates. Precautions were taken for the measurements to be as close as possible to the steady state (for further details see Ramos *et al.*[6]).

As frequently done in the MR literature, results shown in this manuscript correspond to *apparent* stress values (using the stress-torque relationship valid for Newtonian fluids). "Correcting" the torque data using the Weissenberg-Rabinowitsch capillary equation analogue for parallel disks, very slightly shifts the curves to lower stress levels and does not affect the succeeding discussion. Under the assumption that the MR fluids follow a Bingham constitutive equation the difference is in a factor $4/3$.

Rheograms for CMRFs did not exhibit a high-shear viscosity plateau under field. Several attempts were performed to reach it by using highly viscous Newtonian carriers (up to 790 Pa.s). However the high-shear viscosity plateau was still not observable. In this work, we estimated the high-shear viscosity using the Quemada expression: $\eta_\infty = \eta_c(1-\phi/\phi_a)^{-2}$, where ϕ_a is the maximum packing fraction. Here, we assumed a Random Close Packing fraction for spheres, $\phi_a = 0.64$. As we will see latter, this resulted in a reasonably good estimation of the high-shear viscosity in view of the scaling curves (c.f. Figure 3).

7. Results and discussion

Figure 1 represents typical steady shear rheograms for 20 vol% CMRFs at different external magnetic fields. Experimental data are shown for stress-controlled and strain-controlled tests demonstrating a reasonably good collapse in steady regime, as otherwise expected. Although not shown in this manuscript, rheograms were also

Soft Matter Accepted Manuscript

obtained for other particle concentrations giving qualitatively similar results. The rheograms exhibit three clearly differentiated regions: i) an initial region with a noticeable noise because of the limited torque resolution of the magnetorheometer, ii) a plateau in the stress as expected in yield-stress materials, and iii) an increase in stress at large Mn corresponding to the flow region.

In Figure 1a we show scaling curves within the linear and *saturation* regimes according to Equations [7b and 5b] and [7c and 6b], respectively. The curves tend to collapse for the lowest field strengths (below 665 kA/m). Deviations in the collapse are due to the fact that this particular MR fluid is actually not dilute and hence a perfect scaling is not expected. The perfect scaling does not occur because single-width particle chains do not necessarily exist at this concentration (e.g. see Figure 9 in Fernández-Toledano *et al.*[10]). As expected, a better scaling was observed for particle concentrations below 20 vol% (results not shown here for brevity). Interestingly, the curve corresponding to 665 kA/m (that is very close to saturation as we will demonstrate later) is clearly below measurements in the linear regime. This suggests that other interparticle interactions (remanence, short range attractions, colloidal interactions, etc ...) exist between the particles, that become noticeable at low fields, by increasing the stress level. These interactions have been already reported in the literature, for instance, under the frame of a two-step yielding.[10] Interestingly, when the magnetic field strength increases up to saturation, magnetostatic forces govern and therefore the stress curves stay below those corresponding to the linear regime.

In Figure 1b we show the rheograms in dimensionless form now using Equations [7a and 4]. The calculation of $\tau_{mag,<M>}$ and $Mn_{<M>}$ requires the computation of the

Soft Matter Accepted Manuscript

magnetization of the particle $\langle M_p \rangle$ using the internal magnetic field strength H instead of the external one H_0. For the calculation of the internal magnetic field strength we used the expression: $H = \frac{3\mu_{cr}}{\mu_{pr} + 2\mu_{cr}} H_0$, that corresponds to the internal field in an isolated and magnetically linear spherical particle (see section 5.11 in reference 25). Here, μ_{pr} and μ_{cr} were calculated from the experimental magnetization curves using the MM approximation. The process required a self-consistent approach: (i) the internal magnetic field was calculated using the magnetic permeabilities for the external magnetic field, (ii) the magnetization was calculated by interpolation in the magnetization curve, (iii) the magnetic permeabilities for the internal field were calculated, (iv) the steps (ii) and (iii) were repeated until convergence. The magnetization and the internal magnetic field were thus obtained. The inspection of Figure 1b reveals that, as expected, the collapse in the linear regime is now much better than in Figure 1a (note that there are not free fitting parameters), and *saturation* values (at 665 kA/m) still remain clearly below the data corresponding to the linear regime, as previously discussed, because of the presence of other interparticle interactions.

Rheograms for IFFs are represented in Figure 2. The scaling in the linear and saturation regimes is shown in Figure 2a. Obviously, the scaling with the magnetic field strength for IFFs is even better than in the case of CMRFs for the same particle concentration. A very good collapse is found for all magnetic field strengths investigated because in this case $\langle M_p \rangle \approx 3\beta H_0$ in a very wide range of magnetic fields in agreement with Ruiz-López *et al.*[8] (we will come back later to this point in the discussion of Figure 4). The good collapse with measurements on CMRFs at 665 kA/m (i.e. very close to saturation) also reinforces the statement that other interparticle

Soft Matter Accepted Manuscript

interactions exist in CMRFs that appear at low fields (c.f. Figure 2a). Contrary to the case of CMRFs, IFFs tend to exhibit a low-shear viscosity plateau instead of an apparent yield stress. For more details on the appearance of this low-shear viscosity plateau we refer to Berli and de Vicente[11]. Together with experimental data we also show the predictions of Equation [12] in Figure 2a. As expected a very good agreement is found. In Figure 2b we show the stress versus Mason number curves scaled by $\tau_{mag_{<M>}}$ and $Mn_{<M>}$ under the MM approximation. The good scaling demonstrates that the MM approximation is valid in these systems and solely magnetostatic and hydrodynamic interactions play a role, contrary to CMRFs where other interparticle interactions exist.

Next, rheograms contained in Figures 1 and 2 are plotted in the form of dimensionless viscosity curves for a direct comparison to theoretical models, using the mean magnetization of the particles. Results are shown for 20 vol% MR fluids in Figure 3. They demonstrate again that the MM approximation works reasonably well for a wide range of external magnetic field strengths from 17 kA/m to 265 kA/m in both MR fluids investigated, independently of the obvious physical differences in the magnetization mechanism of the suspensions. The shift towards the right in the viscosity curves for the lowest fields, when compared to saturation, is again a consequence of the existence of other interparticle interactions. In agreement with Figure 2, data for IFFs collapse reasonably well with CMRFs at fields close to saturation. From the inspection of Figure 3 we can appreciate again the difficulty in identifying the high-shear viscosity plateau in CMRFs and justifies the use of Quemada expression to estimate it (see Experimental section). The good scaling obtained

Soft Matter Accepted Manuscript

demonstrates that taking the viscosity from this particular analytical expression is a reasonable approximation.

Curves similar to those shown in Figure 3 were also measured for a wide range of concentrations in both CMRFs and IFFs. The collapse was similarly good to the 20 vol% example reported in this work. Once the viscosity curves were measured for a given concentration at a range of magnetic field strengths, a Casson plastic model (Equation [10]) was fitted to obtain the critical Mason number Mn^* associated to the transition from magnetostatic to hydrodynamic control of the suspension structure.

At this point, it is important to highlight that for a very wide range of particle loadings, the mean magnetization of a particle in suspension is not dependent on the particle loading: $\langle M_p \rangle \neq \langle M_p \rangle(\phi)$. This is clearly appreciated in Figure 4 for both CMRFs and IFFs. This finding means that the magnetic stress τ_{mag} is proportional to the particle volume fraction because in its derivation we assumed a linear dependence of the particle area with concentration: $A_p \propto \phi$ (see Equation [7] and Annex). The later assumption is valid in a wide range of experimental data for IFFs. However, in the case of CMRFs this assumption is only valid at very low concentrations (see below). Bearing in mind that in dilute systems $\tau_y \propto \tau_{mag}$ and $\eta_\infty \approx \eta_c$, in view of Equation [11] the MM approximation predicts a linear dependence of the critical Mason number Mn^* with the particle concentration.

To test this prediction we now discuss the volume fraction dependence of the critical Mason number Mn^*. The scaling for the linear ($\mathrm{Mn}^*_{\mathrm{L}}$) and saturation

Soft Matter Accepted Manuscript

(Mn^*_{sat}) approximations gave very similar results to $Mn^*_{<M>}$. As expected, a slightly better collapse was observed for $Mn^*_{<M>}$. Hence, in this discussion we will focus on the scaling of $Mn^*_{<M>}$. Results obtained for the critical Mason number $Mn^*_{<M>}$ as a function of particle concentration ϕ are contained in Figure 5. We observe that the stress-controlled and strain-controlled tests provide very similar numbers giving also an estimate of the consistency of the fitting to the Berli and de Vicente model (Equation [10]). IFFs closely follow a straight line of slope one in very good agreement with the MM approximation for a very wide range of particle loadings (up to 20 vol%); the larger the particle concentration, the larger the number of single-width particle chains per unit surface. As a result this will promote a linearly increasing τ_y and Mn^* with concentration. Together with our data on IFFs we also include data from Ramos *et al.*[6] These data are in reasonably good agreement with our data on IFFs. Our simulation data are also contained in Figure 5 and demonstrate again a linear dependence with volume fraction. This was expected because the MM approximation is employed in the simulations and because only magnetostatic interactions are considered between Hard Spheres. Interestingly the simulation results are very close to experiments on IFFs in spite of the many simplifications in the simulation model. This was expected in view of Ruiz-López *et al.*[8]

In Figure 5 we also include experimental data on CMRFs both in the linear ($H_0 \in [17kA/m, 265kA/m]$) and saturation ($H_0 = 665kA/m$) regimes. In the low concentration regime (below 5 vol%), results collapse very well with simulations and experiments on IFFs. This was expected because the MM approximation becomes exact in this limit. However, results for CMRFs in the linear regime are clearly higher than in saturation for particle loadings above 5 vol%. The reason for this is that other

Soft Matter Accepted Manuscript

contributions to the yield stress τ_y play a role in the linear regime in agreement with the discussion of Figure 1. This gives a stronger than linear dependence of τ_y with ϕ. Mn^* data for saturated CMRFs are obviously closer to those obtained in IFFs because dipolar magnetostatic interactions prevail. However, data for CMRFs do not exactly overlap onto IFFs suggesting that complete saturation is not fully reached in CMRFs (c.f. Figure 4).

For even larger concentrations a maximum with particle concentration is observed because of two contributions to Mn^*: on the one hand, for larger concentrations, the high-shear viscosity contribution to Mn^* becomes more important and therefore, according to Equation [11a] the volume fraction dependence reduces as follows: $\eta_c/\eta_\infty = (1-\phi/\phi_a)^2$. On the other hand, when the volume fraction increases, the permeability of the carrier fluid μ_{cr} in Equation [11a] must be replaced by the permeability of the suspension μ_{sr}. This is so because μ_{sr} will become closer and closer to the permeability of the particles when increasing the concentration. Hence, the τ_y and Mn^* will decrease with the particle loading because the magnetostatic interactions will decrease as well.

At this point it is worth to remark that we explored different possibilities in the calculation of the Mason number for the saturated CMRFs (Equation [6b]). In particular, we explored three cases: i) the suspension magnetization was directly measured in a magnetorheometer, ii) the suspension magnetization was calculated using $M_{susp} = \phi\langle M_p \rangle$ from magnetization measurements in carbonyl iron powders, and iii) the suspension magnetization was calculated again using $M_{susp} = \phi\langle M_p \rangle$ from Frohlich-

Soft Matter Accepted Manuscript

Kennelly equation fittings to magnetization curves in carbonyl iron powders. Results for the three cases demonstrate that the particular way of calculating the suspension magnetization in saturation was negligible in the results presented in this work.

Overall, Figure 5 suggests that even though the MM approximation is not strictly applicable to these systems, it is still a very good approximation for IFFs and it is also valid for CMRFs in both the dilute case and saturation regimes.

Finally, in Figure 6 we show the dimensionless yield stresses as a function of the dimensionless mean magnetization of the particles $\langle M_p \rangle / M_{sat}$. This figure allows us to evaluate the theoretical quadratic dependence predicted by Equation [7] in dilute MR fluids. In Figure 6a we include the static yield stresses as obtained from the low-shear stress plateau in log-log representation (see Figures 1 and 2). In the case of the IFFs, an *apparent static yield stress* is estimated using two approaches (tangent method[6] and the stress level at $\dot{\gamma} = 0.1 s^{-1}$). In both kinds of MR fluids a quadratic dependence with the particle magnetization is observed suggesting that the MM approximation is valid. In fact, under the assumption that $\tau_y \approx \tau_{mag}$, from Equation [7] we get $\tau_y / \tau_{y,sat} = \langle M_p \rangle^2 / M_{sat}^2$. This equation is plotted as a solid line in Figure 6a and as observed is in very good agreement with the data.

In Figure 6b we show results for the dynamic yield stress obtained by fitting the shear stress as a function of the shear rate in lin-lin representation, for shear rates above $100 s^{-1}$. In the case of CMRFs, it was necessary to work under strain-controlled mode to increase the number of points for better statistics in the fittings (see Experimental

Soft Matter Accepted Manuscript

section). In this case, the data clearly deviate and do not superimpose although the slope seems to be still 2. In our opinion, a key point to understand the deviation of the data on the dynamic yield stress is the fact that extrapolations are done on a narrow range of shear rates (or stresses) and the high-shear viscosity is hardly ever achieved in CMRFs. These results are coherent with the shift towards the right in the viscosity curves for the lowest fields observed in Figure 3 as a consequence of the existence of other interparticle interactions. As expected, for the largest fields investigated and the lower concentrations the agreement is much better with data on IFFs and theoretical predictions.

8. Conclusions

The mean magnetization (MM) approximation has been tested against conventional MR fluids (CMRFs) and inverse ferrofluids (IFFs). Results demonstrate that although the approximation is not strictly valid in the field strength and concentration range of general interest, and in spite of the physical differences in the magnetization mechanism of the suspensions, the approximation is still applicable in some particular cases. In IFFs the MM approximation applies very well for all magnetic field strengths and concentrations studied. However, in the case of CMRFs the MM approximation is only applicable in the dilute regime and/or magnetic saturation.

Acknowledgements

This work was supported by MAT 2013-44429-R project (Spain) and by Junta de Andalucía P10-RNM-6630, P10-FQM-5977 and P11-FQM-7074 projects (Spain). J.A.R.-L. acknowledges the financial support by the “Ministerio de Educación: Becas del Programa de Formación del Profesorado Universitario (FPU)” (AP2010-2144).

Soft Matter Accepted Manuscript

J.C.F.-T. acknowledges the Interuniversity Attraction Poles Programme (IAP 7/38 MicroMAST) of the Belgian Science Policy Office for the financial support.

Soft Matter Accepted Manuscript

References

1 J. Rabinow, *AIEE Trans.*, 1948, **67**, 1308–1315.

2 A. T. Skjeltorp, *Phys. Rev. Lett.*, 1983, **51**, 2306-2309.

3 R. E. Rosensweig, *Ferrohydrodynamics*, Dover, New York, 1997.

4 B. J. de Gans, H. Hoekstra and J. Mellema, *Faraday Discuss.*, 1999, **112**, 209–224.

5 J. Ramos, J. de Vicente and R. Hidalgo-Álvarez, *Langmuir*, 2010, **26**(12), 9334-9341.

6 J. Ramos, D. J. Klingenberg, R. Hidalgo-Álvarez and J. de Vicente, *J. Rheol.*, 2011, **55**, 127-152.

7 J. de Vicente, D. J. Klingenberg and R. Hidalgo-Álvarez, *Soft Matter*, 2011, **7**, 3701-3710.

8 J. A. Ruiz-López, J. C. Fernández-Toledano, D. J. Klingenberg, R. Hidalgo-Álvarez and J. de Vicente, *J. Rheol.*, 2015, (in press).

9 J. P. Segovia-Gutiérrez, C. Berli and J. de Vicente, *J. Rheol.*, 2012, **56**(6), 1429-1448.

10 J. C. Fernández-Toledano, J. Rodríguez-López, K. Shahrivar, R. Hidalgo-Álvarez, L. Elvira, F. Montero de Espinosa and J. de Vicente, *J. Rheol.*, 2014, **58**(5), 1507-1534.

11 C. L. A. Berli and J. de Vicente, *Appl. Phys. Lett.*, 2012, **101**(2), 021903-1-4.

12 D. J. Klingenberg, J. C. Ulicny and M.A. Golden, *J. Rheol.*, 2007, **51**, 883-893.

13 M. Ocalan, *Magnetorheological fluids for extreme environments: stronger, lighter, hotter*, Ph. D. Thesis, Massachusetts Institute of Technology, 2011.

14 F. Vereda, J. de Vicente, J. P. Segovia-Gutiérrez and R. Hidalgo-Álvarez, *J. Appl. Phys.*, 2011, **110**, 063520.

Soft Matter Accepted Manuscript

15 F. Vereda, J. P. Segovia-Gutiérrez, J. de Vicente and R. Hidalgo-Álvarez, *J. Phys. D: Appl. Phys.*, 2015, **48**, 015309.

16 L. C. Marshall, F. Zukoski and J. Goodwin, *J. Chem. Soc., Faraday Trans.*, 1989, **85**, 2785-2795.

17 J. M. Ginder and L. C. Davis, *Appl. Phys. Lett.*, 1994, **65**, 3410-3412.

18 J. E. Martin and R. A. Anderson, *J. Chem. Phys.*, 1996, **104**(12), 4814–4827.

19 J. de Vicente, M. T. López-López, J. D. G. Durán and F. González-Caballero, *Rheol. Acta*, 2004, **44**, 94-103.

20 O. Volkova, G. Bossis, M. Guyot, V. Bashtovoi and A. Reks, *J. Rheol.*, 2000, **44**, 91-104.

21 J. C. Fernández-Toledano, J. A. Ruiz-López, R. Hidalgo-Álvarez and J. de Vicente, *J. Rheol.*, 2015, **59**(2), 475-498.

22 H. G. Lagger, T. Breinlinger, J. G. Korvink, M. Moseler, A. Di Renzo, F. Di Maio and C. Bierwisch, *J. Non-Newtonian Fluid Mech.*, 2015, **218**, 16-26.

23 J. R. Melrose and D. M. Heyes, *J. Chem. Phys.*, 1993, **98**(7), 5873-5886.

24 J. P. Segovia-Gutiérrez, J. de Vicente, R. Hidalgo-Alvarez and A. M. Puertas, *Soft Matter*, 2013, **9**, 6970-6977.

25 J. D. Jackson, *Classical Electrodynamics (3rd Edition)*, Wiley & Sons, New York, 1999.

Soft Matter Accepted Manuscript

Annex: Estimation of the area per particle

The estimation of the area per particle was achieved assuming the following statements: First, the MR fluid is assumed to be formed by single-width particle chains, and confined in a plate-plate configuration with upper and lower area, A, and a gap between the plates, h. The volume fraction can be expressed as the volume of all the particles divided by the total volume of the suspension:

$$\phi = \frac{N_p V_p}{V} = \frac{4\pi N_p a^3}{3Ah} \qquad [A1]$$

Here N_p is the number of particles in the sample, V_p is the particle volume, a is the particle radius and $V = Ah$ is the total volume of the MR fluid. Assuming gap-spanning single-width particle chains, the number of chains, N_C, can be written as $N_C = 2aN_p/h$. In terms of stress, the total force is going to be exerted on the surfaces by the upper or the lower particles. So, the area per particle, A_p can be obtained as the total area divided by the number of chains and all the particles have a surrounding area distributed in shells around the fluid in cylindrical symmetry:

$$A_p = \frac{A}{N_c} = \frac{Ah}{2aN_p} = \frac{2\pi a^2}{\phi} \qquad [A2]$$

Soft Matter Accepted Manuscript

Figures:

Fig. 1.- Dimensionless shear stress ($\tau/\tau_{mag,L}$, $\tau/\tau_{mag,sat}$, $\tau/\tau_{mag,<M>}$) curves as a function of the Mason number (Mn_L , Mn_{sat} , $Mn_{<M>}$) for CMRFs at 20 vol% concentration: a) scaled by the linear magnetostatic stress, $\tau_{mag,L}$ and saturated magnetostatic stress, $\tau_{mag,sat}$ as a function of Mn_L and Mn_{sat} ; b) scaled by the mean magnetization magnetostatic stress, $\tau_{mag,<M>}$ as a function of $Mn_{<M>}$. These rheograms were constructed using both strain-controlled (closed symbols) and stress-controlled (open symbols) modes. Labels correspond to the external magnetic field strength.

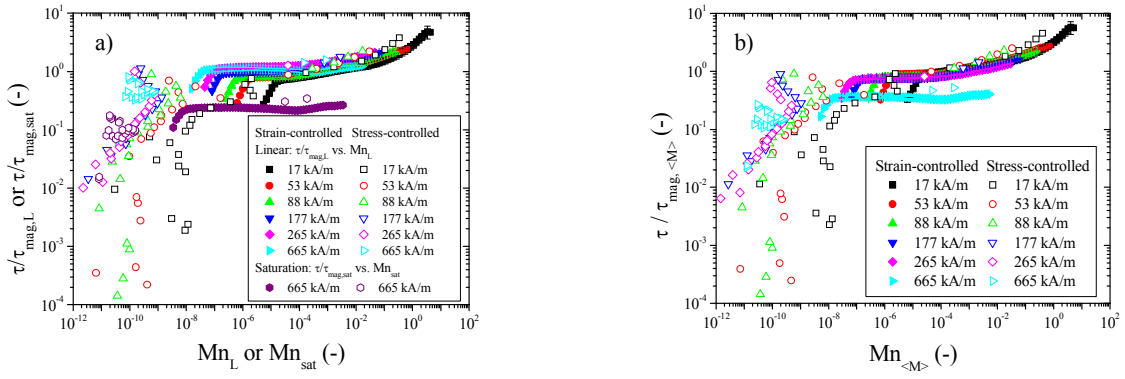

Soft Matter Accepted Manuscript

Fig. 2.- Dimensionless shear stress ($\tau/\tau_{mag,L}$, $\tau/\tau_{mag,sat}$, $\tau/\tau_{mag,<M>}$) curves as a function of the Mason number (Mn_L , Mn_{sat} , $Mn_{<M>}$) for IFFs at 20 vol% concentration: a) scaled by the linear magnetostatic stress, $\tau_{mag,L}$ and saturated magnetostatic stress, $\tau_{mag,sat}$ as a function of Mn_L and Mn_{sat} ; b) scaled by the mean magnetization magnetostatic stress, $\tau_{mag,<M>}$ as a function of $Mn_{<M>}$. These rheograms were constructed using stress-controlled mode. Labels correspond to the external magnetic field strength. Solid and dashed lines correspond to Equation [12] for IFFs and CMRFs in saturation regime, respectively.

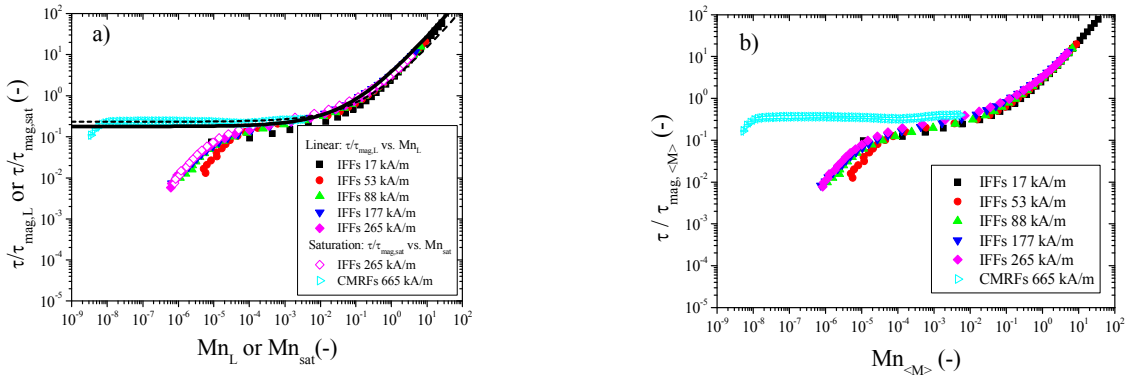

Soft Matter Accepted Manuscript

Fig. 3.- Dimensionless viscosity η curves (scaled by the high-shear viscosity η_∞ of the MR fluid) as a function of Mason number $Mn_{<M>}$ for MR fluids at 20 vol% reported in Figures 1 and 2. For CMRFs the high-shear viscosity is taken from the Quemada expression (see text).

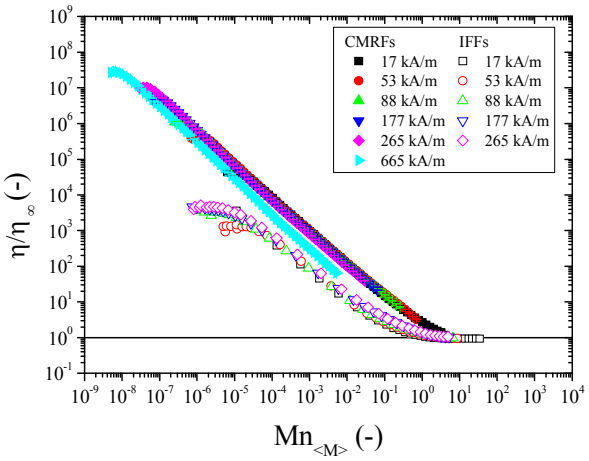

Soft Matter Accepted Manuscript

Fig. 4.- Mean magnetization of the particle $\langle M_p \rangle$ scaled with the saturation magnetization as a function of the external magnetic field strength H_0 for different particle loadings ϕ in CMRFs (closed symbols) and IFFs (open symbols). For details on the self-consistent approach used to calculate $\langle M_p \rangle$ we refer to the text. M_{sat} = 1707 kA/m for CMRFs and M_{sat} = 25.5 kA/m for IFFs.

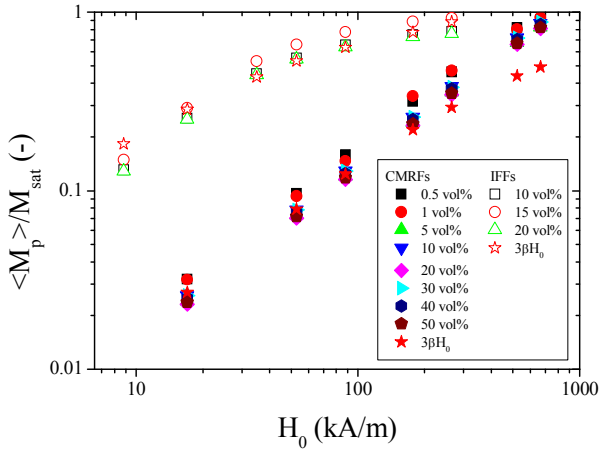

Soft Matter Accepted Manuscript

Fig. 5.- Volume fraction dependence of the critical Mason number $Mn^{*}_{<M>}$ for CMRFs and IFFs as obtained by fitting the dimensionless viscosity curves to the Casson model (Equation [10]). In these fittings the high-shear viscosity for the CMRFs is taken from the Quemada equation and for the IFFs is taken from the high-shear viscosity in the absence of fields during the preshear.

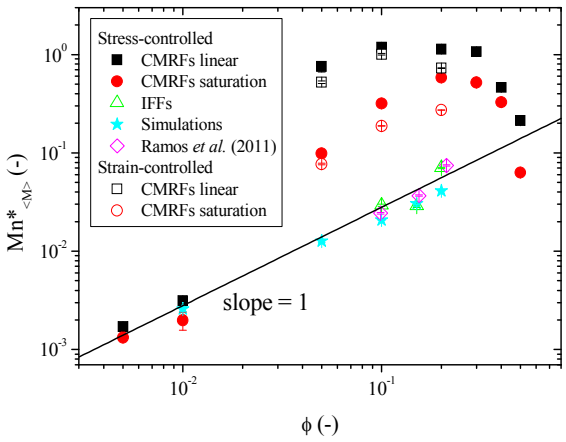

Soft Matter Accepted Manuscript

Fig. 6.- Particle magnetization dependence of the static $\tau_{y,static}$ (a) and dynamic $\tau_{y,dynamic}$ (b) yield stresses, normalized by the yield stress in saturation $\tau_{y,sat}$. Particle magnetization $< M_p >$ was normalized by the saturation magnetization M_{sat}. Solid line corresponds to the theoretical prediction $\tau_y / \tau_{y,sat} = \langle M_p \rangle^2 / M_{sat}^2$. Open symbols in Figure 6a: $\dot{\gamma} = 0.1 s^{-1}$. Crossed open symbols in Figure 6a: tangent method.

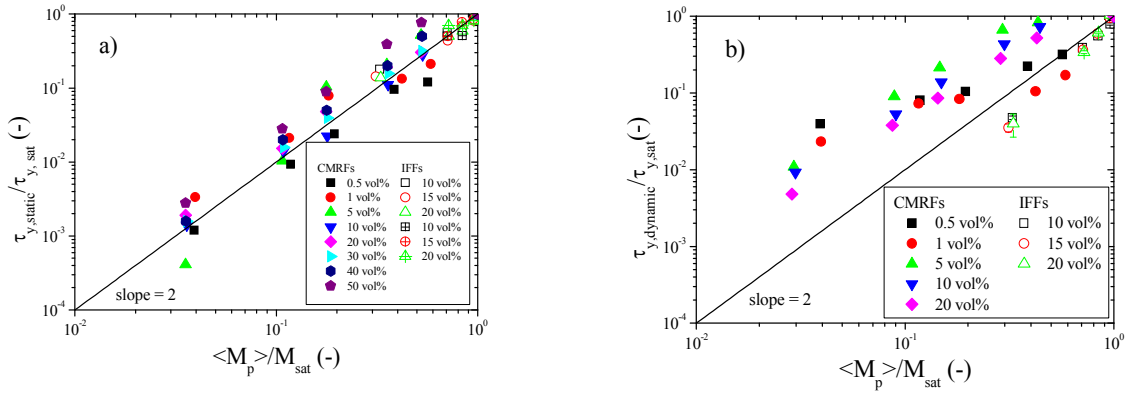

Soft Matter Accepted Manuscript